
Universiteit
Leiden
The Netherlands

Folic acid modified mesoporous silica nanoparticles for cellular and nuclear targeted drug delivery

Porta, F.; Lamers, G.E.; Morrhayim, G.; Chatzopoulou, A.; Schaaf, M.J.M.; Dulk, H. den; ... ; Kros, A.

Citation
Porta, F., Lamers, G. E., Morrhayim, G., Chatzopoulou, A., Schaaf, M. J. M., Dulk, H. den, ... Kros, A. (2013). Folic acid modified mesoporous silica nanoparticles for cellular and nuclear targeted drug delivery. *Advanced Healthcare Materials*, *2*(2), 281-286. doi:10.1002/adhm.201200176

Version:	Publisher's Version
License:	Licensed under Article 25fa Copyright Act/Law (Amendment Taverne)
Downloaded from:	https://hdl.handle.net/1887/3665021

Note: To cite this publication please use the final published version (if applicable).

Folic Acid-Modified Mesoporous Silica Nanoparticles for Cellular and Nuclear Targeted Drug Delivery

*Fabiola Porta, Gerda E. M. Lamers, Jess Morrhayim, Antonia Chatzopoulou, Marcel Schaaf, Hans den Dulk, Claude Backendorf, Jeffrey I. Zink, and Alexander Kros**

Site-specific stimuli delivery systems are attractive materials as drug-delivery systems (DDSs) for the treatment of cancer disease in which the ultimate goal is the release of significant amount of drug in selected areas without damaging the surrounding healthy cells.[1] Therefore, the drug carrier must possess a number of properties such as biocompatibility with a living environment; high loading capacity of the drug; prevention of any premature release, the ability to target specific cancer cells, and controlled release.[1b,2] In the last decade, a wide variety of DDSs have been explored, based upon dendrimers, hydrogels, liposomes, and inorganic nanoparticles.[3] However, mesoporous inorganic nanomaterials represent a good candidate for drug delivery as they preserve the payload from the metabolism and the immune response for a longer period of time. Therefore, the distribution of the nanocarrier in all of the districts of the organism reaching the targeted site and releasing a significant concentration of drug can be achieved.[1b,4] In order to accomplish targeting and tunable release, inorganic nanoparticles have to undergo surface modification.[5]

Mesoporous silica nanoparticles (MSNs) are actively studied materials for drug delivery because of their fascinating properties.[6] These nanomaterials were evaluated in vivo, and high biocompatibility was observed.[6b] Moreover, the pore size can be varied thereby allowing the loading of guest molecules with different molecular weights and variable steric hindrance. The organic modification of the nanocarrier surface transforms the nanomaterial into a "smart" drug-release device where the valve has three important functions: to prevent any premature release, to deliver the payload upon a specific stimulus in order to avoid any side effects, and to target the system towards a specific cell type.[7]

In order to prevent aggregation in aqueous media, hydrophilic valves have been designed composed of peptides,[8] antibodies,[9] DNA/dendrimers complexes and lipid bilayers.[9b] In this paper we studied a new stimuli-responsive material based on silica mesoporous nanoparticles capped with rotaxane valves and a folic acid head group. The nanovalve system consists of a monolayer of mechanically interlocked molecules in the form of the rotaxane composed of: a linear stalk anchoring the rotaxane on the surface, a gating ring that encircles it and locks the cargo in the mesopores, and a stopper located at the end of the linker, connected to it with a cleavable bond.[6a] Herein, the so-called rotaxane nanovalves are activated by esterase enzymes while the targeting moiety, folic acid, is an integral part of the valve system. Folic acid, the soluble form of vitamin B, targets tumors in a similar manner to monoclonal antibodies, as folate receptors (FRs) are overexpressed in more than 40% of human tumors,[10] but are generally absent in healthy cells.[11]

We previously used silica-modified nanoparticles with folic acid in order to increase the selectivity towards cancer cells. However, in these studies the folic acid was not a part of a nanovalve system.[12]

The rotaxane structures locks the guest molecules in the pores while preventing any premature leakage. The folic acid moiety is an integrated part of the rotaxane structure (**Scheme 1**). Nanoparticles loaded with the anticancer drug camptothecin (CPT) were evaluated as a drug-release system in cell cultures, and their effect on the apoptosis mechanism of the cells was studied with Western Blot and terminal deoxynucleotidyl transferase dUTP nick end labeling (TUNEL) staining assays.

Folic acid-modified mesoporous silica nanoparticles (FAMSNs) were synthesized from tetraethyl orthosilicate (TEOS) using hexadecyltrimethylammonium bromide (CTAB) as a surfactant template agent.[1b,13] Scanning electron microscopy (SEM) showed that the particles were spherical with an average diameter of 200 nm. The surfactant was subsequently removed from the pores refluxing with acidic methanol and the CTAB removal was confirmed by Fourier transformed infrared (FTIR) spectroscopy (see Supporting Information, Figure S1). The inner pores have an average diameter of 2.8 nm and the channels are aligned, as confirmed by transmission electron microscopy (TEM) and X-ray diffraction (XRD) (**Figure 1**).

Dr. F. Porta, J. Morrhayim, Dr. A. Kros
Leiden Institute of Chemistry
Soft Matter Chemistry
Leiden University
Einsteinweg 55, 2333 CC, Leiden, The Netherlands
E-mail: a.kros@chem.leidenuniv.nl
G. E. M. Lamers, A. Chatzopoulou, Dr. M. Schaaf
Institute of Biology
Molecular Cell Biology
Leiden University
Einsteinweg 55, 2333 CC, Leiden, The Netherlands
H. den Dulk, Dr. C. Backendorf
Leiden Institute of Chemistry
Molecular Genetics
Leiden University
Einsteinweg 55, 2333 CC, Leiden, The Netherlands
Prof. J. I. Zink
Department of Chemistry and Biochemistry
University of California
Los Angeles, CA 90095, USA

DOI: 10.1002/adhm.201200176

© 2013 WILEY-VCH Verlag GmbH & Co. KGaA, Weinheim

ADVANCED HEALTHCARE MATERIALS
www.advhealthmat.de

www.MaterialsViews.com

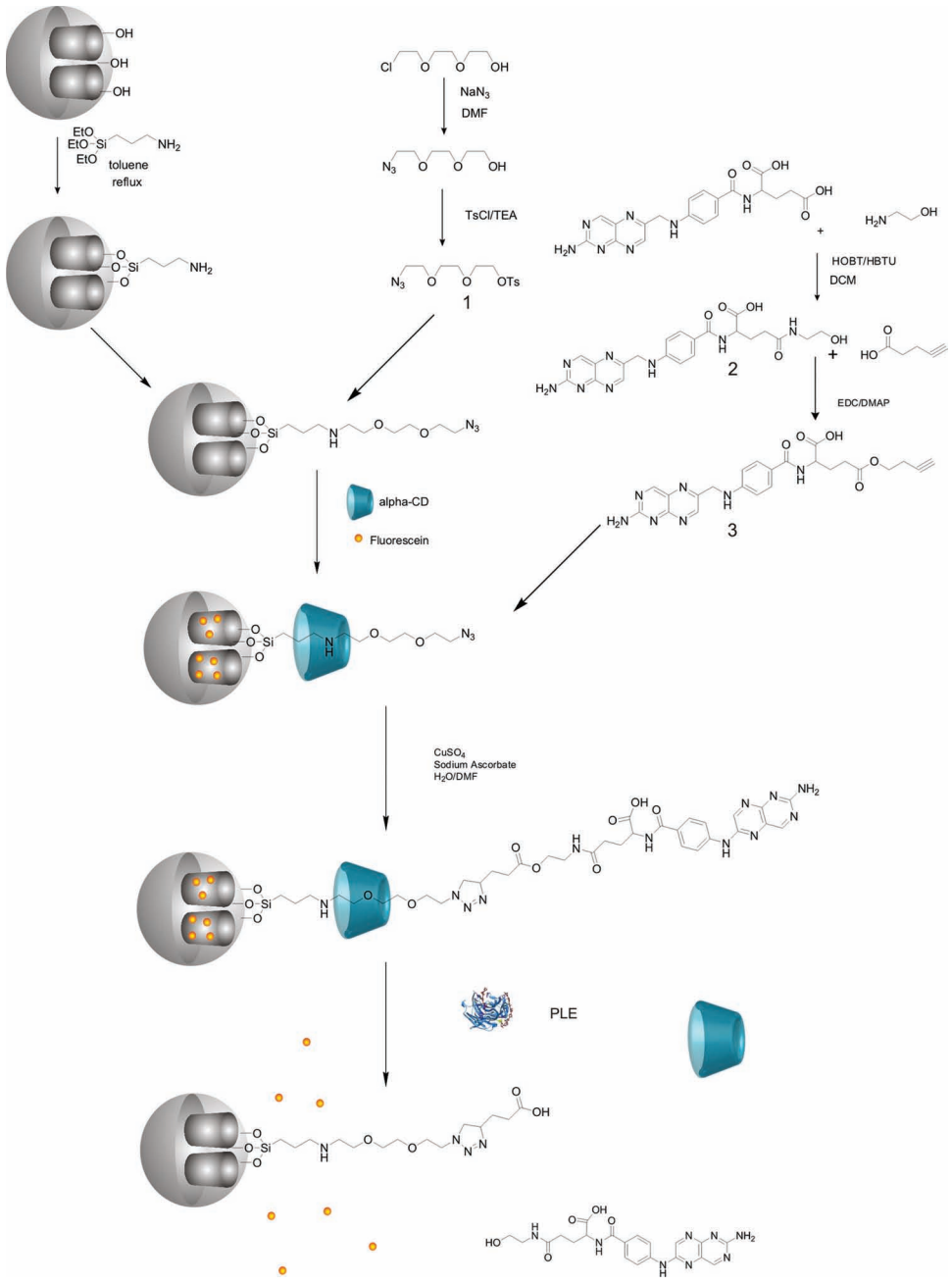

Scheme 1. Synthesis of the folic acid silica nanoparticles (FAMSNs): the particles are loaded with fluorescein which is released upon bioactivation of the valve towards porcineliver esterase (PLE).

For the construction of the nanovalve at the silica nanoparticles the folic acid was modified with ethanolamine (**2**) and coupled with pentynoic acid for the introduction of an alkyne moiety (**3**) as shown in Scheme 1.[14] Next, the mesoporous silica nanoparticles (MSNs) modified with an azide terminus (**4**) were modified with the folic acid moiety using a copper(I)-catalyzed click reaction.

The prevention of uncontrolled release of drugs before reaching the desired targeted cell is an important property of a drug-delivery system. Therefore we investigated the release of fluorescein, a model compound for our kinetic studies. The nanoparticles were loaded with 5×10^{-3} M solution of fluorescein overnight and capped with the rotaxane and the folic acid moiety. Next, the nanosystem was washed three times with phosphate buffer saline (PBS) to remove the excess of fluorescein. Typically, the FAMSNs contained approximately 4.6 nmol of fluorescein per mg of nanoparticles. Next, the release was investigated in vitro in the presence of porcine liver esterase (PLE). Interestingly the release showed a lag-time of 30 min and we hypothesize that the cyclodextrin (α-CD) acts as a steric shield for the ester bond from hydrolysis, which is different compared with earlier work.[7e] In the absence of esterase, the

© 2013 WILEY-VCH Verlag GmbH & Co. KGaA, Weinheim

21922659, 2013, 2, Downloaded from https://onlinelibrary.wiley.com/doi/10.1002/adhm.201200176 by University Of Leiden, Wiley Online Library on [11/10/2023]. See the Terms and Conditions (https://onlinelibrary.wiley.com/terms-and-conditions) on Wiley Online Library for rules of use; OA articles are governed by the applicable Creative Commons License

21922659, 2013, 2, Downloaded from https://onlinelibrary.wiley.com/doi/10.1002/adhm.201200176 by University Of Leiden, Wiley Online Library on [11/10/2023]. See the Terms and Conditions (https://onlinelibrary.wiley.com/terms-and-conditions) on Wiley Online Library for rules of use; OA articles are governed by the applicable Creative Commons License

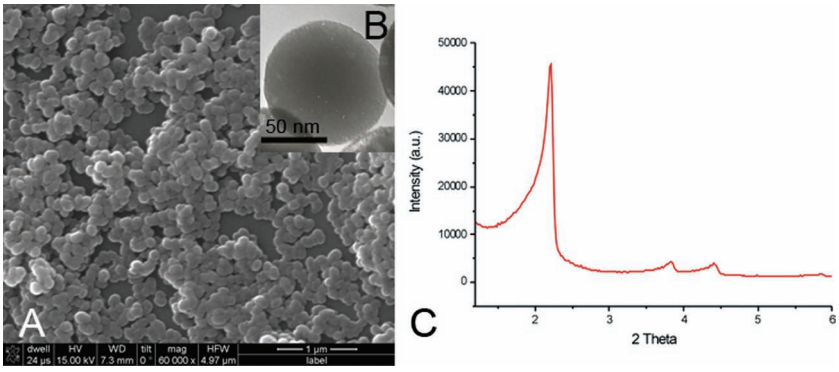

Figure 1. Characterization of the FAMSNs: A) scanning electron microscopy (SEM) of FAMSNs; B) transmission electron microscopy (TEM) image of FAMSNs. C) The nanoparticles show the typical XRD pattern of MCM-41 hexagonal mesoporous silica.

rotaxane structures prevent undesired release of dye showing its effectiveness as a valve system (**Figure 2**). For efficient drug delivery into cells it is necessary that the nanoparticles do not cluster in media as they will lower the cellular uptake. Hence it is important to create a hydrophilic surface and avoid any undesired interactions between the particles. The surface functionalization achieves this goal, because the folic acid moiety gives hydrophilic properties to the nanoparticles and the α-CD prevents aggregation in media. As shown in a previous study,[8] we investigated the importance of the α-CD tethered on an aliphatic stalk when nanoparticles were dispersed in aqueous solutions. The shielding action of the α-CD prevents interparticle aggregation; thus, clustering in physiological media is minimized. Dynamic light scattering (DLS) measurements were performed in order to understand the purpose of the organic functionalization. Silica nanoparticles have the tendency to aggregate in buffered media and therefore strategies have been developed in order to prevent this phenomenon.[5,7b,12b] One of the most exploited methods is the pegylation of the external surface, which precludes clustering effects and without any precipitation in fetal serum.[15] In our case, the organic surface functionalization also precludes aggregation and, at the same time, it functions as an esterase-activated snap-top drug-delivery system. The hydrodynamic radius of unmodified MSNs in PBS buffer indeed indicates clustering of the particles, while FAMSNs were shown to be monomeric (R_h = 517 nm and 196 nm respectively) (**Figure 3**). Thus the presence of this rotaxane structure including the folic acid moiety prevents clusters of the particles effectively and the observed diameter corresponds well with the average size obtained by SEM (approximately 200 nm).

A homogeneous suspension containing fluorescein-loaded FAMSNs (1 μg mL^{-1}) in PBS were incubated with human osteosarcoma U2Os cells for 1 hour in PHEM medium to study the cellular uptake and toxicity. The cells were washed to remove any cell-membrane-adhered FAMSNs and analyzed using confocal laser scanning microscopy. The nuclei of the cells were stained with 4′,6-diamino-2-phenylindole (DAPI) and the cell cytoskeleton was marked with phalloidine-Alexafluor 594. The cells were shown to have green fluorescent nanoparticles in the cytoplasm, revealing that the FAMSNs were taken up by the cancer cells. The presence of nanoparticles was observed in all of the cultured cells analyzed.

The efficiency of FAMSN uptake was quantified by flow cytometry as a function of time showing an increasing internalization of the FAMSNs in cancer cells, while, in the control experiment, unmodified MSNs did not show this trend (**Figure 4**A). In approximately 90% of the U2Os cells endocytosis of FAMSNs was determined. Thus, functionalization with folic acid positively influences the uptake of FAMSNs by cancer cells, indicating that the overexpressed folic acid receptors are involved in the cellular uptake (Figure 4B–D).[10,16] Surprisingly FAMSNs were sometimes also observed in the nuclei of the U2Os cancer cells (Figure 4D). This is remarkable, as the nuclear pore complex (NPC) is typically able to transport

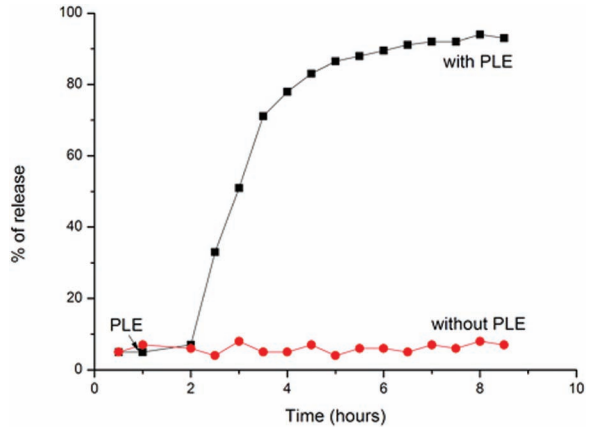

Figure 2. Controlled release of fluorescein in the presence (■) and absence (●) of 0.12 mL porcine liver esterase (PLE) with a concentration of 10 mg mL^{-1} in 3.2 M $(NH_4)_2SO_4$.

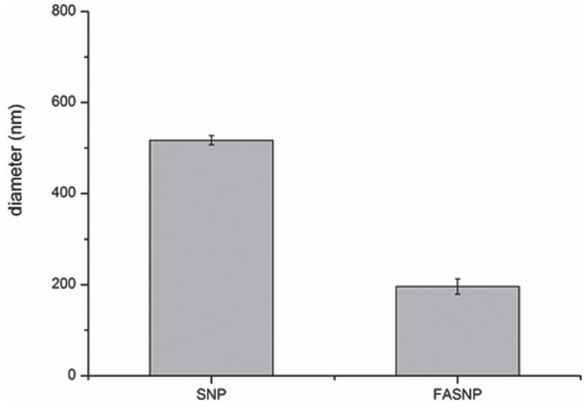

Figure 3. Hydrodynamic diameter of MSNs and FAMSNs determined by dynamic light scattering. The analysis was done in 1 M PBS buffer (pH = 7.24); MSNs aggregate in buffer solution while FAMSNs remain separate and do not aggregate due to surface functionalization.

© 2013 WILEY-VCH Verlag GmbH & Co. KGaA, Weinheim

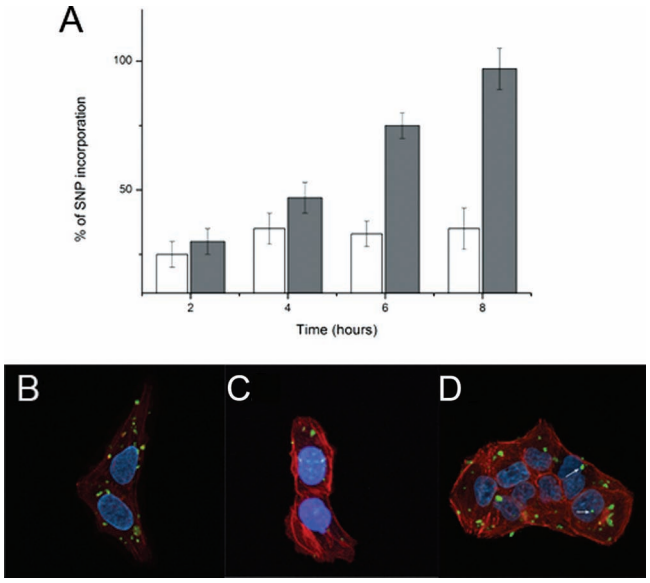

Figure 4. U2Os endocytosis experiment. A) Graph representing the inclusion percentage of FAMSNs (gray bars) versus unmodified mesoporous silica nanoparticles (white bars): due to surface functionalization, the FAMSNs are selectively taken up by the cancer cells, while bare silica nanoparticles do not show this tendency. B) Laser confocal microscopy of U2Os cells with FAMSNs (green). The blue signal is given by the nuclei and the cytoskeleton was stained in red. B,C) U2Os cells with particles located in the cytoplasm. D) The nanoparticles are also visible in the nuclear region, as shown by the white arrows.

20–50 nm particles into the nucleus, depending on the cell line. However, Chen showed that 70 nm SiO_2 particles can be transported through the NPC, while 200 nm particles are unable to enter the nucleus.[17] The diameter of the silica core used in this study was approximately 100 nm, as determined by SEM (Figure 1a). Furthermore, a possible explanation could come from the work of Bozard et al.,[18] who showed the presence of folate receptors in the nuclear membrane. Therefore, our findings are in line with this study, since the FAMSNs are taken up in the nucleus using the receptor-mediated mechanism. To support this hypothesis, we also studied the cellular uptake of unmodified MSNs using the same experimental conditions with confocal laser scanning microscopy, and these nanoparticles were found only in the cytoplasm (Supporting Information, Figure S2).

The drug delivery of camptothecin (CPT) in human cancer cells leads to growth inhibition and cell death. However, CPT is hydrophobic; thus, the formulation and the delivery of this drug remains a challenge. Therefore the delivery of CPT using FAMSNs can increase the efficacy of this molecule, preventing serious side effects as the compound is released only in the targeted cells. When a cancer cell enters the apoptosis pathway there is an activation of several mechanisms that lead the cell to a programmed death. Activation of specific enzymes, such as caspase-3, and the fragmentation of nuclear DNA are the most-investigated pathways.[19]

The release of CPT from the FAMSNs into the cytoplasm was investigated using a TUNEL assay and a Western blot.

CPT-loaded FAMSNs were incubated with U2Os at 37 °C and then fixed after 30, 60, 180, and 240 min. Next, we studied the effect of released CPT on the cell with the TUNEL assay. In **Figure 5**A–C, laser confocal images are reported of samples fixated after 60, 180, and 240 min. The TUNEL-positive cells bear green fluorescence in the nuclear region due to selective interaction of the labeled nick end with fragmented DNA. We determined the percentage of cellular death (TUNEL-positive cells) versus time of incubation and observed 90% of cells were positive after 240 min. Thus folic acid-modified nanocarriers after being taken up by cancer cells, release their payload in an effective manner, as confirmed by the DNA fragmentation of the TUNEL-positive cells. We also investigated whether the MSNs and FAMSNs showed any toxicity. Figure 5E shows the positive TUNEL cells after incubation with MSNs (control), a solution of 5×10^{-3} M of CPT in dimethyl sulfoxide (DMSO),[5] FAMSNs, and CPT-loaded FAMSNs. The MSNs and FAMSNs showed biocompatibility properties when incubated with U2Os cells as only a low cytotoxicity was observed. The effect on the apoptosis of a solution in DMSO of the anticancer drug CPT was observed as approximately 50% of cultured cells were found to be positive. However 93% were found to be positive when exposed to CPT-FAMSNs nanoparticles. This result is very important as the calculated amount of CPT released by the suspension of nanoparticles used for the assay was 0.4 nmol of CPT per μg of FAMSNs: thus, significantly lower than the amount previously used. Therefore, loading nanoparticles with CPT increases significantly the efficacy of this drug, as it is delivered directly in the cellular environment. Moreover, the prevention of any premature release allows the delivery of a significant concentration of CPT at the targeted site.

In summary, we designed a site-specific drug-delivery system using the so-called nanovalve concept. The FAMSNs release their cargo upon a biological stimulus (i.e., esterase) and no leakage was observed in the absence of this enzyme. Thus this system prevents significantly severe side effects due to the unspecific release of the drug. A lag time of approximately 30 min was observed due to the steric hindrance of the tethered rotaxane. Moreover, the cyclodextrin has a crucial role in preventing aggregation, as shown by DLS experiment. Active internalization was observed when folic acid was a part of the surface functionalization of the nanocarrier, as confirmed by flow-cytometry studies. The FAMSNs were demonstrated to be biocompatible as they do not induce apoptosis in U2Os cultured cells. This result was also confirmed by a TUNEL assay where the cytotoxicity was compared with unmodified MSNs. The release of CPT from the FAMSNs was detected and quantified as a function of time using TUNEL and Western Blot assays. Hence, the delivery of the anticancer drug led to the detected pharmacological effects as a significant concentration of the compound was released in the cytoplasm of the cells.

At present, a large number of molecules in the pipeline of pharmaceutical companies have low water solubility and therefore some administration ways are completely precluded.[20] The employment of mesoporous silica nanoparticles to encapsulate hydrophilic anticancer drugs is one of the most promising strategies to deliver these compounds into living organisms. The ability to functionalize the silica surface with specific targeting molecules enhances the possibility of having successful

© 2013 WILEY-VCH Verlag GmbH & Co. KGaA, Weinheim

21922659, 2013, 2, Downloaded from https://onlinelibrary.wiley.com/doi/10.1002/adhm.201200176 by University Of Leiden, Wiley Online Library on [11/10/2023]. See the Terms and Conditions (https://onlinelibrary.wiley.com/terms-and-conditions) on Wiley Online Library for rules of use; OA articles are governed by the applicable Creative Commons License

21922659, 2013, 2, Downloaded from https://onlinelibrary.wiley.com/doi/10.1002/adhm.201200176 by University Of Leiden, Wiley Online Library on [11/10/2023]. See the Terms and Conditions (https://onlinelibrary.wiley.com/terms-and-conditions) on Wiley Online Library for rules of use; OA articles are governed by the applicable Creative Commons License

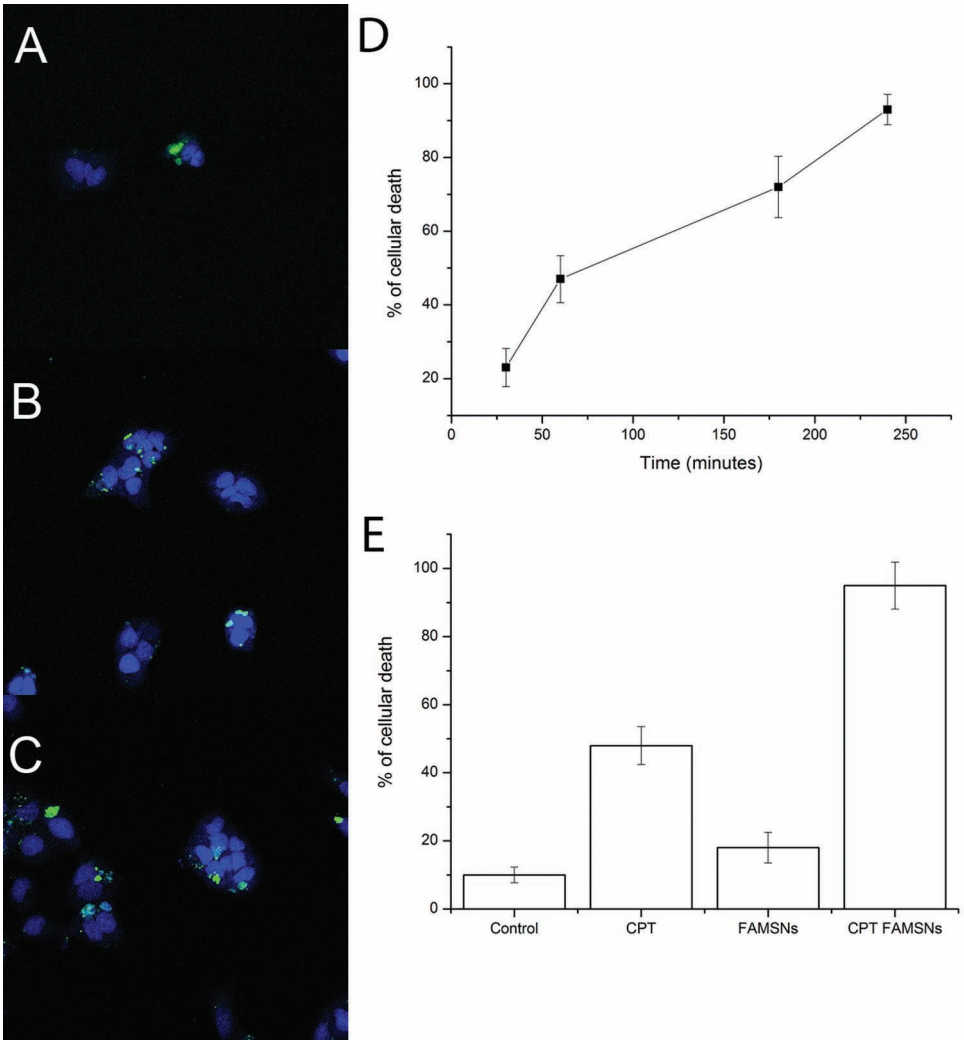

Figure 5. TUNEL staining assay in U2Os cells. U2Os were incubated with FAMSNs loaded with CPT and analyzed using laser confocal scanning microscopy. Positive apoptotic cells have green fluorescent nuclei, while not-apoptotic cells have blue (DAPI) nuclei. A–C) Laser confocal image after 1 hour (A), after 3 hours (B), and after 4 hours (C). D) Amount of positive TUNEL cells as a function of time. After 4 hours of incubation, approximately 90% of the U2Os observed were found to be apoptotic. E) TUNEL assay performed with MSNs (control), FAMSNs, a solution in DMSO of CPT, and FAMSNs loaded with CPT. MSNs and FAMSNs have shown a low cytotoxicity very similar to the normal turnover of a cell culture. 50% of the U2Os cells were found dead after exposure to CPT solution in DMSO, while 93% of the cells were found positive to TUNEL after exposure to CPT-loaded FAMSNs. Thus, the nanoparticles deliver the drug into the cytoplasm releasing an effective amount of CPT.

therapies for cancer diseases and vaccine applications. Further work is necessary to establish these functionalized silica nanoparticles as a tool for selective and targeted release, while minimizing cytotoxic side effects.

Experimental Section

The experimental procedures are reported in the Supporting Information.

Supporting Information

Supporting Information is available from the Wiley Online Library or from the author.

Acknowledgements

The authors acknowledge the support of the Smart Mix Programme of the Netherlands Ministry of Economic Affairs and the Netherlands Ministry of Education, Culture and Science. We also acknowledge Dr. Nabila Bardine and Dr. Nicoletta Gaggero for helpful and practical discussions.

Received: May 22, 2012
Revised: July 10, 2012
Published online: August 28, 2012

[1] a) B. Asadishad, M. Vosoughi, I. Alamzadeh, A. Tavakoli, *J. Dispersion Sci. Technol.* **2010**, *31*, 492–500; b) J. L. Vivero-Escoto, I. I. Slowing, B. G. Trewyn, V. S. Y. Lin, *Small* **2010**, *6*, 1952–1967; c) O. C. Farokhzad, S. Y. Jon, A. Khademhosseini, T. N. T. Tran, D. A. LaVan, R. Langer, *Cancer Res.* **2004**, *64*, 7668–7672.

 © 2013 WILEY-VCH Verlag GmbH & Co. KGaA, Weinheim

[2] I. I. Slowing, B. G. Trewyn, S. Giri, V. S. Y. Lin, *Adv. Funct. Mater.* **2007**, *17*, 1225–1236.
[3] a) U. Boas, P. M. H. Heegaard, *Chem. Soc. Rev.* **2004**, *33*, 43–63; b) R. Haag, F. Kratz, *Angew. Chem. Int. Ed.* **2006**, *45*, 1198–1215; c) W. H. De Jong, P. J. A. Borm, *Int. J. Nanomed.* **2008**, *3*, 133–149; d) E. Soussan, S. Cassel, M. Blanzat, I. Rico-Lattes, *Angew. Chem. Int. Ed.* **2009**, *48*, 274–288; e) V. P. Torchilin, *Curr. Drug Delivery* **2005**, *2*, 319–327; f) V. P. Torchilin, *Biomater. Delivery Targeting Proteins Nucleic Acids* **2005**, 433–459.
[4] a) J. M. Rosenholm, C. Sahlgren, M. Linden, *Nanoscale* **2010**, *2*, 1870–1883; b) M. Vallet-Regi, A. Ramila, R. P. del Real, J. Perez-Pariente, *Chem. Mater.* **2001**, *13*, 308–311; c) J. Lu, M. Liong, Z. X. Li, J. I. Zink, F. Tamanoi, *Small* **2010**, *6*, 1794–1805.
[5] J. Lu, M. Liong, J. I. Zink, F. Tamanoi, *Small* **2007**, *3*, 1341–1346.
[6] a) M. W. Ambrogio, C. R. Thomas, Y.-L. Zhao, J. I. Zink, J. F. Stoddart, *Acc. Chem. Res.* **2011**, *44*, 903–913; b) F. Sharif, F. Porta, A. H. Meijer, A. Kros, M. K. Richardson, *Int. J. Nanomed.* **2012**, *7*, 1875–1890.
[7] a) T. D. Nguyen, K. C. F. Leung, M. Liong, C. D. Pentecost, J. F. Stoddart, J. I. Zink, *Org. Lett.* **2006**, *8*, 3363–3366; b) H. A. Meng, M. Liong, T. A. Xia, Z. X. Li, Z. X. Ji, J. I. Zink, A. E. Nel, *ACS Nano* **2010**, *4*, 4539–4550; c) E. Ruiz-Hernandez, A. Baeza, M. Vallet-Regi, *ACS Nano* **2011**, *5*, 1259–1266; d) J. Lu, E. Choi, F. Tamanoi, J. I. Zink, *Small* **2008**, *4*, 421–426; e) K. Patel, S. Angelos, W. R. Dichtel, A. Coskun, Y. W. Yang, J. I. Zink, J. F. Stoddart, *J. Am. Chem. Soc.* **2008**, *130*, 2382–2383; f) I. I. Slowing, B. G. Trewyn, V. S. Y. Lin, *J. Am. Chem. Soc.* **2006**, *128*, 14792–14793.
[8] F. Porta, G. E. M. Lamers, J. I. Zink, A. Kros, *Phys. Chem. Chem. Phys.* **2011**, *13*, 9982–9985.
[9] a) D. R. Radu, C.-Y. Lai, J. W. Wiench, M. Pruski, V. S. Y. Lin, *J. Am. Chem. Soc.* **2004**, *126*, 1640–1641; b) R. Liu, Y. Zhang, P. Feng, *J. Am. Chem. Soc.* **2009**, *131*, 15128–15129.
[10] P. S. Low, S. A. Kularatne, *Curr. Opin. Chem. Biol.* **2009**, *13*, 256–262.
[11] J. Sudimack, R. J. Lee, *Adv. Drug Delivery Rev.* **2000**, *41*, 147–162.
[12] a) K. Hayashi, M. Moriya, W. Sakamoto, T. Yogo, *Chem. Mater.* **2009**, *21*, 1318–1325; b) M. Liong, J. Lu, M. Kovochich, T. Xia, S. G. Ruehm, A. E. Nel, F. Tamanoi, J. I. Zink, *ACS Nano* **2008**, *2*, 889–896; c) A. Garcia-Bennett, M. Nees, B. Fadeel, *Biochem. Pharmacol.* **2011**, *81*, 976–984; d) J. M. Oh, S. J. Choi, G. E. Lee, S. H. Han, J. H. Choy, *Adv. Funct. Mater.* **2009**, *19*, 1617–1624; e) J. Gu, W. Fan, A. Shimojima, T. Okubo, *Small* **2007**, *3*, 1740–1744; f) L. Sun, Y. Zang, M. D. Sun, H. G. Wang, X. J. Zhu, S. F. Xu, Q. B. Yang, Y. X. Li, Y. M. Shan, *J. Colloid Interface Sci.* **2010**, *350*, 90–98.
[13] a) C. Y. Lai, B. G. Trewyn, D. M. Jeftinija, K. Jeftinija, S. Xu, S. Jeftinija, V. S. Y. Lin, *J. Am. Chem. Soc.* **2003**, *125*, 4451–4459; b) S. Huh, J. W. Wiench, B. G. Trewyn, S. Song, M. Pruski, V. S. Y. Lin, *Chem. Commun.* **2003**, 2364–2365; c) I. I. Slowing, C. W. Wu, J. L. Vivero-Escoto, V. S. Y. Lin, *Small* **2009**, *5*, 57–62.
[14] a) K. Hayashi, K. Ono, H. Suzuki, M. Sawada, M. Moriya, W. Sakamoto, T. Yogo, *Chem. Mater.* **2010**, *22*, 3768–3772; b) A. K. Bose, B. N. Ghoshmazumdar, B. G. Chatterjee, *J. Am. Chem. Soc.* **1960**, *82*, 2382–2386; c) J. C. Sheehan, A. K. Bose, *J. Am. Chem. Soc.* **1951**, *73*, 1761–1765.
[15] a) V. Cauda, C. Argyo, T. Bein, *J. Mater. Chem.* **2010**, *20*, 8693–8699; b) S. R. Blumen, K. Cheng, M. E. Ramos-Nino, D. J. Taatjes, D. J. Weiss, C. C. Landry, B. T. Mossman, *Am. J. Respiratory Cell Mol. Biol.* **2007**, *36*, 333–342.
[16] a) H. Elnakat, M. Ratnam, *Adv. Drug Delivery Rev.* **2004**, *56*, 1067–1084; b) H. Elnakat, M. Ratnam, *Frontiers Biosci.* **2006**, *11*, 506–519.
[17] M. Chen, A. von Mikecz, *Exp. Cell Res.* **2005**, *305*, 51–62.
[18] B. R. Bozard, P. S. Ganapathy, J. Duplantier, B. Mysona, Y. Ha, P. Roon, R. Smith, I. D. Goldman, P. Prasad, P. M. Martin, V. Ganapathy, S. B. Smith, *Invest. Ophthalmol. Visual Sci.* **2010**, *51*, 3226–3235.
[19] a) T. Hashimoto, U. Kikkawa, S. Kamada, *PLoS One* **2011**, *6*, e18449. b) A. K. Frank, E. C. Pietsch, P. Dumont, J. Tao, M. E. Murphy, *Cancer Biol.Therapy* **2011**, *11*, 740–745; c) S. A. Bensasson, Y. Sherman, Y. Gavrieli, *Methods Cell Biol.* **1995**, *46*, 29–39; d) Y. Gavrieli, Y. Sherman, S. A. Bensasson, *J. Cell Biol.* **1992**, *119*, 493–501.
[20] V. Wagner, A. Dullaart, A. K. Bock, A. Zweck, *Nat. Biotechnol.* **2006**, *24*, 1211–1217.

© 2013 WILEY-VCH Verlag GmbH & Co. KGaA, Weinheim

21922659, 2013, 2, Downloaded from https://onlinelibrary.wiley.com/doi/10.1002/adhm.201200176 by University Of Leiden, Wiley Online Library on [11/10/2023]. See the Terms and Conditions (https://onlinelibrary.wiley.com/terms-and-conditions) on Wiley Online Library for rules of use; OA articles are governed by the applicable Creative Commons License